Retrospective Correction of WM Inhomogeneity and Brain Extraction of MR Images

Robert Dahnke[1], Christian Gaser[1]
1 - Structural Brain Mapping Group, Department of Psychiatry / Neurology, Jena University Hospital, Germany

INTRODUCTION

Advantages of higher field strength scanners come along with increased intensity inhomogeneity or bias (Belaroussi 2006; Vovk 2007) that require retrospective correction due to individual dependencies (Manjon 2007).

Here we present a new, robust, accurate and reliable inhomogeneity correction for T1 weighed brain MR images. The iterative process uses a local maximum filter within a stepwise-reconstructed white matter (WM) segment to approximate the bias field. For WM estimation a brain extraction routine and a k-means classifier is used.

For validation the coefficient of variation (CV) and the tissue segments were compared to N3 (Sled 1998; Boyes 2008), N3 with FSL BET (Smith 2002) and FSL FAST, and SPM8 (new segment, Ashburner 2005) for simulated and real MR images. SVE (Segmentation Validation Engine - Shattuck 2009) was used for evaluation of the brain extraction.

METHODS

The algorithm starts with a noise correction (Manjon 2010), assuming that "image = bias * scan + noise" (Sled 1998).

The bias correction process contains two main components, a fast initial bias correction and brain extraction, and the final iterative bias correction procedure (Fig. 1).

The initial bias correction starts with a rough maximum-based bias correction of all low frequency objects at a resolution of around 16 mm. This allows the coarse identification of the major part of WM, as the biggest, high intensity, and low gradient region of the head at 4 mm resolution. A region growing is used to complete the brain-mask and a k-means estimation identifies the cerebrospinal fluid (CSF), gray matter (GM), and WM peaks on a resolution of 2 mm. The WM segment is used for the final maximum-based bias correction at 4 mm.

The iterative part now refines the WM segmentation to avoid overestimation in high intensity GM structures, like the basal ganglia. Furthermore, bias field smoothness is accommodated to the estimated strength of the initial correction with a low regularization for strong fields and a high regularization for low fields. The process runs until the changes of the coefficient of variation (CV) is below 0.001.

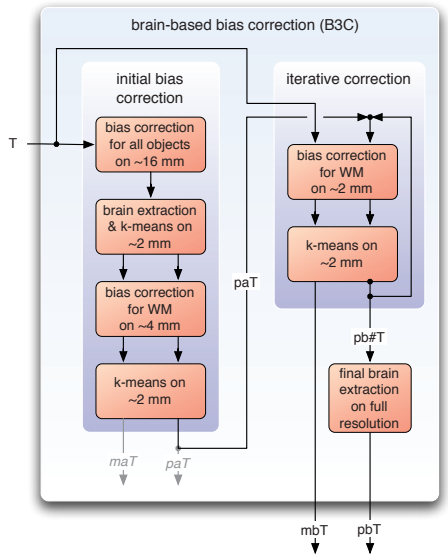

Fig. 1 Flow diagram of the brain-based bias correction (B3C) algorithm. An initial rough maximum-based bias correction of all low frequency objects of an input image (T) is used to find the brain and its tissue classes (paT) for the second bias correction (left). This segment map is refined in an iterative process (pb#T) (right). The final bias corrected image (mbT) and the final segmentation (pb#T) are used for the final brain extraction (pbT).

The CV was estimated for an eroded WM segment to avoid partial volume effects (PVE) on the GM/WM boundary.

Only the WM segment was used, because the GM segment is often affected by the PVE, depends on the subject age, and contains real intensity variations in regions like the basal ganglia, the motor cortex or the occipital lobe. After the inhomogeneity correction the final brain extraction is performed.

RESULTS

24 simulated images of Brain Web Phantom (BWP) (Collins 1998) with varying noise (3% and 9%), fields (A, B, and C) and field strength (±40% and ±100), were used for basic evaluation (Fig. 2).

The generated tissue segments have a good agreement with the ground truth segments (Fig. 3). Low segmentation results of FSL depend strongly on inaccurate skull-stripping of BET.

Brain extraction was tested with the SVE with quite good results for an algorithm without any prior maps (Jaccard: 0.940 ± 0.010, Dice 0.9695 ± 0.005, Sensitivity: 0.998 ± 0.001, Specificity: 0.952 ± 0.013).

Calculation times depend on the image size and inhomogeneity, but were typically below 3 minutes on a standard computer (initialization ~30s + iterations ~90s + final brain extraction ~ 60s).

Figure 4 shows 3 examples of the original and the images corrected using our method. For higher field strength (7T) further improvements are necessary to avoid local undercorrections in fine structures and overcorrections in subcortical structures.

A

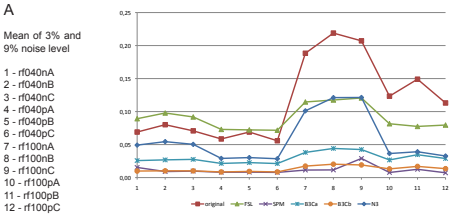

B

	CV(eWM)	CV(GM)	CV(WM)	CV
Original	0,117 ± 0,058	0,176 ± 0,063	0,130 ± 0,059	0,153 ± 0,060
B3C (init - maT)	0,030 ± 0,013	0,081 ± 0,009	0,038 ± 0,010	0,060 ± 0,009
B3C (final - mbT)	0,013 ± 0,006	0,087 ± 0,005	0,027 ± 0,004	0,057 ± 0,003
FSL	0,043 ± 0,024	0,091 ± 0,022	0,052 ± 0,024	0,071 ± 0,022
N3	0.051 ± 0.045	0.115 ± 0.042	0.063 ± 0.044	0.090 ± 0.043
SPM	0,012 ± 0,009	0,072 ± 0,006	0,027 ± 0,007	0,049 ± 0,006

Fig. 2 Results of the inhomogeneity correction for the brain web phantom. Figure A shows the mean CV of the eroded WM segment (CV(eWM)) for both noise levels. Figure B shows the mean and standard deviation of the CV for different segments.

A

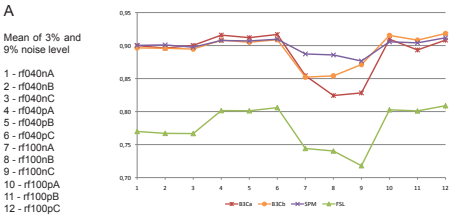

B

	kappa (CSF)	kappa (GM)	kappa (WM)	kappa (GM+WM)
FSL	0,556 ± 0,046	0,694 ± 0,090	0,760 ± 0,095	0,938 ± 0,024
SPM	0,704 ± 0,065	0,827 ± 0,074	0,852 ± 0,066	0,922 ± 0,010
B3C (init - maT)	0,727 ± 0,051	0,834 ± 0,066	0,851 ± 0,075	0,961 ± 0,005
B3C (final - mbT)	0,711 ± 0,016	0,849 ± 0,058	0,873 ± 0,051	0,950 ± 0,019

Fig. 3 Segmentation results of the inhomogeneity correction for the brain web phantom.

CONCLUSIONS

B3C was able to produce exact and stable results for a wide set of test data. It outperforms N3 and FSL, and yields similar results to SPM, without using prior information that can produce errors for atypical anatomy. The skull stripping showed good performance.

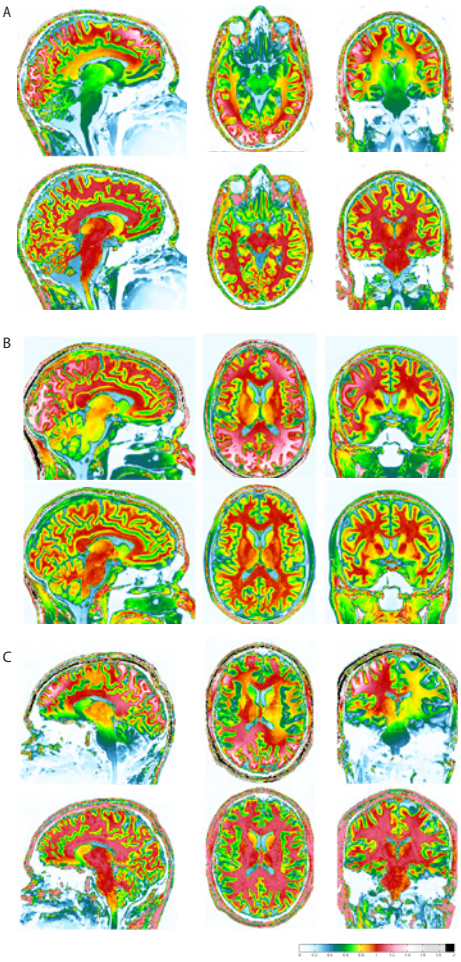

Fig. 4 Shown are the noise corrected T1 images (top row), and the results of the B3C bias correction (bottom row) for three example images with 3.0T (A,B) and 7.0T (C).

ACKNOWLEDGEMENTS

Robert Dahnke and Christian Gaser are supported by the German BMBF grants 01EV0709.

REFERENCES

Ashburner, J. and K. J. Friston (2005). "Unified segmentation." Neuroimage 26(3): 839-851.

Belaroussi, B., J. Milles, et al. (2006). "Intensity non-uniformity correction in MRI: existing methods and their validation." Med Image Anal 10(2): 234-246.

Boyes, R. G., J. L. Gunter, et al. (2008). "Intensity non-uniformity correction using N3 on 3-T scanners with multichannel phased array coils." Neuroimage 39(4): 1752-1762.

Collins, D. L., A. P. Zijdenbos, et al. (1998). "Design and construction of a realistic digital brain phantom." IEEE Trans Med Imaging 17(3): 463-468.

Manjon, J. V., P. Coupe, et al. (2010). "Adaptive non-local means denoising of MR images with spatially varying noise levels." J Magn Reson Imaging 31(1): 192-203.

Manjon, J. V., J. J. Lull, et al. (2007). "A nonparametric MRI inhomogeneity correction method." Med Image Anal 11(4): 336-345.

Shattuck, D. W., G. Prasad, et al. (2009). "Online resource for validation of brain segmentation methods." Neuroimage 45(2): 431-439.

Sled, J. G., A. P. Zijdenbos, et al. (1998). "A nonparametric method for automatic correction of intensity nonuniformity in MRI data." IEEE Trans Med Imaging 17(1): 87-97.

Smith, S. M. (2002). "Fast robust automated brain extraction." Hum Brain Mapp 17(3): 143-155.

Vovk, U., F. Pernus, et al. (2007). "A review of methods for correction of intensity inhomogeneity in MRI." IEEE Trans Med Imaging 26(3): 405-421.

E-mail: robert.dahnke@uni-jena.de

PDF of the poster is available at: http://dbm.neuro.uni-jena.de/HBM2013/Dahnke01.pdf